Chapter 8

Modelling of methane production and emissions

Keshab Sharma[1], Oriol Gutierrez[2], Zhiguo Yuan[1], Matthijs R. J. Daelman[3], Mark C. M. van Loosdrecht[3] and Eveline I. P. Volcke[4]

[1]*Advanced Water Management Centre, The University of Queensland, St. Lucia, Queensland, Australia. E-mail: keshab@awmc.uq.edu.au; zhiguo@awmc.uq.edu.au*
[2]*Catalan Institute of Water Research (ICRA), Girona, Spain. E-mail: ogutierrez@icra.cat*
[3]*Department of Biotechnology, Delft University of Technology, Delft, the Netherlands. E-mail: matthijs.daelman@gmail.com; M.C.M.vanLoosdrecht@tudelft.nl*
[4]*Department of Green Chemistry and Technology, Ghent University, Belgium. E-mail: Eveline.Volcke@UGent.be*

SUMMARY

This chapter provides a review of the models available for estimating the production and emission of methane from wastewater collection and treatment systems. The details of a number of mechanistic models as well as the simplified empirical models have been summarized. Their limitations have been identified and general methods for calibration and validation have been presented.

Keywords: Activated sludge, emission, methane, model, oxidation, production, sewer

TERMINOLOGY

Term	Definition
Greenhouse gas	Gas that absorbs and emits radiant energy within the thermal infrared range.
Collection system	A system of sewer pipes that collects wastewater from different sources and delivers it to a wastewater treatment plant
SeweX	A dynamic model for simulating hydrogen sulfide and methane generation in a sewer system
Sulfate reducing bacteria (SRB)	A group of bacteria found in anaerobic biofilm, which can perform anaerobic respiration utilizing sulfate as the terminal electron acceptor and reducing it to hydrogen sulfide. Organic carbon is generally used as the electron donor.
Methanogens	A group of microorganisms (archaea) that produce methane as a metabolic by-product under anaerobic conditions.

Methanotrophs	Prokaryotes that metabolize methane as their source of carbon and energy. They can be either bacteria or archaea and can grow aerobically or anaerobically. These require single-carbon compounds to survive.
Model calibration	A process of adjustment of the model parameters to obtain a model representation of the processes of interest that satisfies prescribed criteria.
Model validation	A process by which model outputs are systematically compared to independent real-world observations to judge the quantitative and qualitative correspondence with reality.
Anaerobic digestion	A biochemical process through which microorganisms break down organic matter in the absence of oxygen generating methane-rich biogas.
Empirical model	A model based on statistical relationships between the output and inputs, which are developed using experimental data.
Dissolved methane	Methane (CH_4) gas present in dissolved form in the water phase.
Activated sludge process	A wastewater treatment process for treating sewage or industrial wastewaters using aeration and biological flocs composed of bacteria and protozoa.

8.1 INTRODUCTION

Modelling of methane production in wastewater systems emerged from the modelling of anaerobic digestion, in which the production of methane gas has been the major focus. The methane model for anaerobic digestion has been widely reported in literature. However, due to the continuous evolution of sewer models during the past 3 decades and renewed interest in greenhouse gas (GHG) emissions from the collection systems, there has been significant development in methane modelling for sewer systems. It is not only the production, but also the consumption of methane, which serves as a sink for methane, that has attracted the interest of many researchers in recent years. This has led to the development of models for methane removal in aerobic systems, primarily the aerobic methane oxidation. This chapter summarizes the models for methane production and removal in an urban wastewater system.

8.2 CH$_4$ MODELLING FOR COLLECTION SYSTEM

Due to the operational complexity of sewer systems and dynamic nature of methane production as well as emissions, it is not practical to estimate overall CH_4 emissions from large sewer networks through either online or offline measurements presented in the earlier chapters. Mathematical modelling of the methanogenic activity is a viable option for predicting the methane production and emission in sewer networks. A mathematical model also serves as a powerful tool for the water industry, supporting operational optimization and the development of mitigation strategies for GHG emission control from their collection systems. To date, a number of different models for predicting methane production in sewers have been developed. These models are described in the following sections.

8.2.1 Mechanistic model for CH$_4$ production in sewer biofilms

Guisasola *et al.* (2009) developed a mechanistic model for CH_4 production in sewer biofilms, which has been incorporated in the sewer model presented in Sharma *et al.* (2008) to account for the methanogenic activity. The sewer model, which is now known as the SeweX model (Cesca *et al.*, 2015; Nguyen *et al.*, 2015), is a dynamic sewer model, describing in-sewer biological, chemical, and physical processes. It predicts both the temporal and spatial variations of wastewater characteristics, including sulfate, sulfide and methane, using sewer network configuration, pipe geometry, sewage characteristics and hydraulic data as the inputs. SeweX is the first sewer model capable of predicting the spatial and temporal variation in dissolved and gas phase methane concentrations in a sewer system.

The processes included in the sewer CH_4 model are listed in Table 8.1, while a schematic presentation of these processes is shown in Figure 8.1. The following processes that are responsible for methane production in sewers are included in the SeweX model.

1. Acidogenesis
2. Acetogenesis
3. Acetoclastic methanogenesis
4. Hydrogenotrophic methanogenesis
5. Acetate-based sulfidogenesis
6. Hydrogenotrophic sulfidogenesis
7. Propionate-based sulfidogenesis

The Monod type kinetic expressions are used for the biofilm-catalysed processes and higher values of saturation constants are employed to account for substrate diffusion limitations in the biofilm. Some of the key features of this model are:

1. The sewer biofilm is considered the main contributor to sulfide and methane production.
2. Fermentation is modelled considering the acetate, propionate, and hydrogen as the products.
3. Acetoclastic methanogenesis is the predominant mechanism for methane production.
4. Glucose has been used to represent the fermentable substrates in the biochemical reactions as in Anaerobic Digestion Model No. 1 (ADM1, Batstone *et al.*, 2002).
5. Given the fact that direct propionate utilization by methanogens is not possible and propionate in real sewage is at a low concentration, propionate is considered as an electron donor only for sulfate reduction, not for methane generation.
6. The fermentative bacteria are likely to outcompete sulfate reducing bacteria (SRB) for the fermentable substrates (e.g., sugars or other carbohydrates). For this reason, sulfate reduction using these substrates is not considered in the model and the use of these substrates by SRB is accounted for by considering the use of the fermentation products from these substrates.

The details of the stoichiometric and kinetic parameters included in the SeweX model, which describe the interactions between sulfate reducing bacteria, fermentative bacteria (FB) and methanogenic archaea (MA) can be found in Guisasola *et al.* (2009).

The SeweX model with parameters initially calibrated using the data collected from lab-scale experiments (Guisasola *et al.*, 2009), was subsequently validated using manually sampled, offline methane data from two sewer sites, one in Australia and another in Spain. Figure 8.2 shows a comparison of measured CH_4 data (offline) with the model predicted results for a sewer system in Australia (Guisasola *et al.*, 2009), while Figure 8.3 shows a similar comparison for a sewer system in Spain. Figure 8.4 compares a long-term field CH_4 measurement (online) data from another sewer system in Australia (Liu *et al.*, 2015b) with the CH_4 results predicted using the calibrated model. These comparisons clearly demonstrate the validity of the sewer CH_4 model discussed above.

Although the model predictions and field data showed very good correlations in the above presented cases, more online field measurement data are needed for further calibration and validation of the methane related kinetics, especially under a wide range of sewer conditions.

8.2.2 Methane oxidation under aerobic environment

Despite there being a strong possibility of methane oxidation under aerobic conditions in a gravity sewer by methanotrophs, there is no information on this available in the literature. The lack of sufficient information suggests that there has been no attempt made so far to model the methane oxidation in gravity sewers. Modelling efforts have been focused only on the anaerobic sewer biofilm in the rising main, which is the source of methane in a sewer system.

Table 8.1 Stoichiometry and kinetics of the model describing the interactions among MA, FB and SRB (Guisasola *et al.*, 2009).

Process	CH_4 (Methane)	$C_2H_4O_2$ (Acetate)	$C_6H_{12}O_6$ (Glucose)	$C_3H_6O_2$ (Propionate)	CO_2	H_2	H_2O	H_2SO_4	H_2S	Kinetics
	mol/L									
Hydrogenotrophic methanogenesis	1				−1	−4	2			$k_{CH_4,H_2} \cdot \dfrac{S_{H_2}}{K_{H_2,MA} + S_{H_2}} \cdot \dfrac{A}{V} \cdot \alpha^{T-20}$
Acetoclastic methanogenesis	1	−1			1					$k_{CH_4,SAc} \cdot \dfrac{S_{AC}}{K_{S_{AC},MA} + S_{AC}} \cdot \dfrac{A}{V} \cdot \alpha^{T-20}$
Acetogenesis		2	−1		2	4	−2			$q_{ACETOG} \cdot \dfrac{S_F}{K_F + S_F} \cdot \dfrac{A}{V} \cdot \alpha^{T-20}$
Acidogenesis		2	−3	4	2		2			$q_{ACIDOG} \cdot \dfrac{S_F}{K_F + S_F} \cdot \dfrac{A}{V} \cdot \alpha^{T-20}$
Hydrogenotrophic sulfidogenesis						−4	4	−1	1	$k_{H_2S,H_2} \cdot \dfrac{S_{H_2}}{K_{H_2,SRB} + S_{H_2}} \cdot \dfrac{S_{SO_4}}{K_{SO_4} + S_{SO_4}} \cdot \dfrac{A}{V} \cdot \alpha^{T-20}$
Acetate-based sulfidogenesis		−1			2		2	−1	1	$k_{H_2S,SAc} \cdot \dfrac{S_{AC}}{K_{AC,SRB} + S_{AC}} \cdot \dfrac{S_{SO_4}}{K_{SO_4} + S_{SO_4}} \cdot \dfrac{A}{V} \cdot \alpha^{T-20}$
Propionate-based sulfidogenesis		1		−1	1		2	−3/4	3/4	$k_{H_2S,SProp} \cdot \dfrac{S_{PROP}}{K_{PROP,SRB} + S_{PROP}} \cdot \dfrac{S_{SO_4}}{K_{SO_4} + S_{SO_4}} \cdot \dfrac{A}{V} \cdot \alpha^{T-20}$

Figure 8.1 Schematic representation of the methane biological model. Sulfate reducing bacteria processes (solid line), fermentative bacteria processes (dash–dotted line) and methanogenic archaea processes (dashed line) (Guisasola *et al.*, 2009).

8.2.3 Methane production in sewer sediments

Liu *et al.* (2015a) developed a detailed, but simple, one-dimensional sediment model to predict methane and sulfide production and microbial distribution in a sewer sediment based on the biological reactions proposed by Guisasola *et al.* (2009). The proposed model is presented in Equation (8.1).

$$r_{CH4} = k \times S_F^{0.5} \tag{8.1}$$

where, r_{CH4} is the areal methane production rate (g CH_4/m^2·day); k is the rate constant for methane production expressed as (g CH_4/m)$^{0.5}$/day; and S_F is the bulk fermentable chemical oxygen demand (COD) concentration (mg/L).

Figure 8.2 SeweX model predictions vs offline CH_4 data collected from a sewer system in Australia (Guisasola *et al.*, 2009).
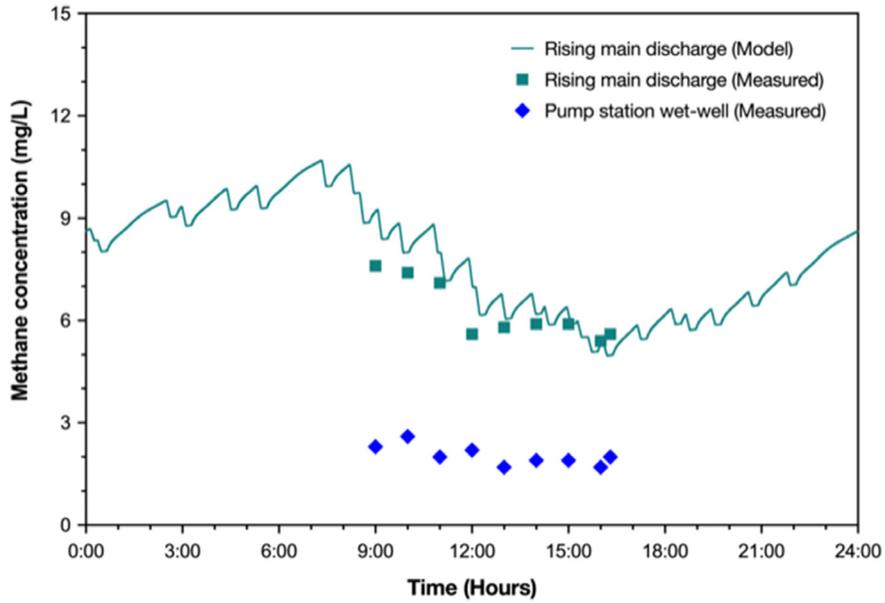
Figure 8.3 SeweX model predictions vs measured CH$_4$ data (off-line) for a sewer system in Spain.
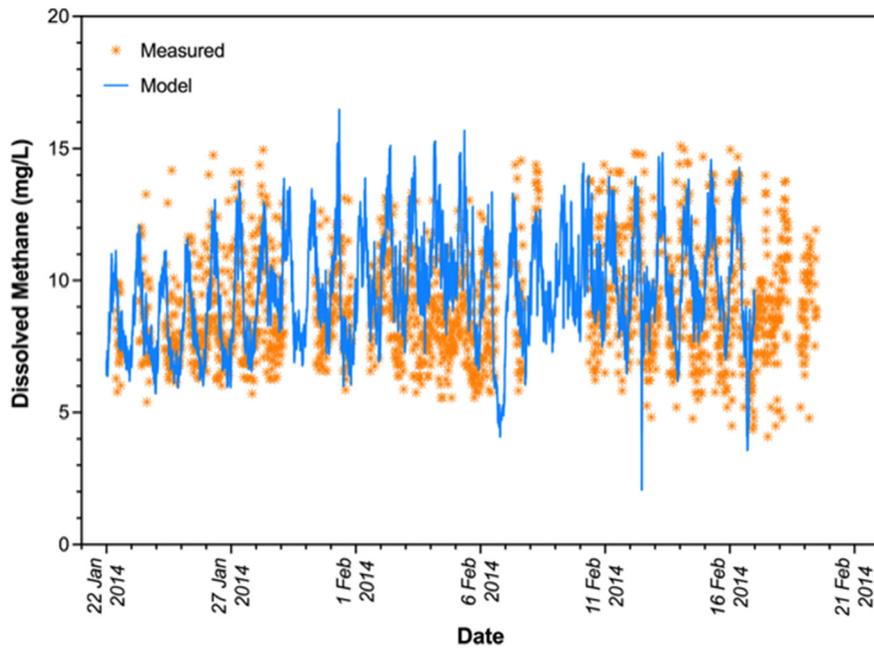

Figure 8.4 Calibrated seweX model predictions vs measured CH$_4$ data (on-line) for a sewer system in Australia.

The parameter k was calibrated using the least squares method after comparing the model predicted methane production rate with the measured value under different substrate concentrations. A value of 0.224 ± 0.002 was obtained for k with the R^2 estimate of 0.99. The model presented in Equation (8.1) has been found to describe the methane production in sewer sediment under different flow velocity (shear stress) conditions (Liu *et al.*, 2016).

The proposed half-order kinetic model can be easily used in the determination of the contribution of sewer sediments to the overall sewer network emissions. The model is very simple as it involves only one parameter to be calibrated that is, k. However, more field data is required to examine the accuracy of the proposed model and understand the dependency of k on key sewer conditions including the sediment properties and wastewater characteristics.

8.2.4 Empirical models predicting methane production in sewers

The mechanistic model for CH_4 production described in Section 8.2.1 requires a large amount of data and is not suitable for quick CH_4 estimation for a sewer pipe. Alternatively, an empirical model could be a useful tool in such a case.

Foley *et al.* (2009) proposed a simple empirical model for estimating CH_4 production in a rising main sewer using data collected from Australian sewers. This simple empirical model represented a correlation of measured CH_4 data from a limited number of rising main sewers with the pipe properties and hydraulic conditions (Equation (8.2)). It was intended for application to similar rising mains with 'similar operational characteristics', which included temperature and organic matter content of the wastewater. The model was a best fit of measured dissolved CH_4 production to hydraulic residence time (HRT) and the ratio of biofilm area to water volume in the sewer.

$$C_{CH4} = 5.24 \times 10^{-5} \times \left(\frac{A}{V} \times \mathrm{HRT} \right) + 0.0015 \tag{8.2}$$

where C_{CH4} is the concentration of dissolved methane (kg/m³); 5.24×10^{-5} kg/m²/h represents the rate of methanogenic activity of the pipeline biofilm; and 0.0015 kg/m³ is the average residual concentration of dissolved methane. This empirical model is based on field observations and considers that the CH_4 production is a function of the wastewater HRT and the biofilm area to water volume (A/V) ratio of the pipe. This simple equation offers a valuable tool for water authorities to predict methane emissions from a rising main sewer. It should be noted that the methane production rate (5.24×10^{-5}) is expected to be affected by many other factors such as the wastewater composition (specifically the COD concentration) and temperature, and it likely varies from system to system. Therefore, more field data is required to further calibrate and validate this empirical model for its generalized application.

With regard to gravity sewers, Chaosakul *et al.* (2014) developed an empirical model to predict methane formation in gravity sewers based on the A/V ratio, HRT and wastewater temperature (Equation (8.3)). The model parameters were estimated using the field data collected in central Thailand.

$$C_{CH4} = 6.0 \times 10^{-5} \times \left(\frac{A}{V} \times \mathrm{HRT} \right) \times 1.05^{(T-20)} + 0.0015 \tag{8.3}$$

where C_{CH4} is the concentration of dissolved methane (kg/m³); 6.0×10^{-5} kg/m²/h is the rate of methanogenic activity of the pipeline biofilm; 0.0015 kg/m³ is the average residual concentration of dissolved methane; and $1.05^{(T-20)}$ is a function of temperature (in °C). This model has been calibrated with measured methane data from the field and partially validated using rising main sewer data. However, the fit of the model predictions with the measured data was poor as R^2 was found to be only 0.06, which is very low. A number of different possible reasons, including limited range of A/V and HRT used in the study, and variation in weather conditions, have been postulated for this observation. By comparing the two equations presented here for rising main and gravity sewer, respectively, it appears that the gravity sewers in Thailand would produce more CH_4 than the rising main sewers in Australia for the same HRT and A/V ratio, which itself is quite surprising.

Xu *et al.* (2018) attempted to further improve the model proposed by Chaosakul *et al.* (2014) by introducing a biomass term and removing the A/V ratio term as shown in Equation (8.4).

$$Q_{CH4} = Y_{CH4/x} \cdot X \cdot HRT \cdot 1.05^{(T-20)} \tag{8.4}$$

where Q_{CH4} is the methane production in mg/L·day; $Y_{CH4/x}$ is the yield coefficient (mg methane/kg biomass); and X is the amount of biomass (kg). The biomass amount is estimated by considering the wall shear-stress, which depends upon sewer slope, degree of fullness of sewer flow, and velocity of flow. The details of the equations used for estimating the biomass amount can be found in Xu *et al.* (2018).

None of the three empirical equations described above consider the impacts of substrate concentration (COD), and this could lead to some errors in methane prediction.

Recently, Water Research Foundation (WRF) has published a methodology for sewer methane estimation in the form of a technical report (Willis *et al.*, 2020). In an attempt to develop the tools for the quantification of methane emissions from gravity as well as the rising main sewers, separate empirical equations taking into account the key field variables such as wastewater flow, pipe diameter, slope and temperature have been proposed for the gravity and rising main sewers. These equations have been developed using the data generated from a large number of simulations with the SeweX model for a range of the variables representing a wide variety of sewer design conditions. The parameters of the model were estimated by carrying out regression and fitting the parameter values to minimize the sum of the square of errors among the two data sets.

The proposed equation for the prediction of methane production in a gravity sewer is:

$$r_{CH_4} = 0.419 \cdot 1.06^{(T-20)} \cdot Q^{0.26} \cdot D^{0.28} \cdot S^{-0.138} \tag{8.5}$$

where, r_{CH_4} is the methane production rate (kg/km·day); Q is the average flow over a day (m³/s); D is the pipe diameter (m); and S is the pipe slope (m/m).

The equation for the estimation of methane production in a rising main sewer is:

$$r_{CH_4} = 3.45 \cdot 1.06^{(T-20)} \cdot D \cdot N_P^{0.202} \cdot 0.396^{(1-N_P \times P_I/1440)} \tag{8.6}$$

where, r_{CH_4} is the methane production rate (kg/km·day); T is the temperature (°C); D is the pipe diameter (m); N_P is the number of pumping events per day; and P_I is the average pumping interval (min). This equation could be used for intermittently running and continuously running rising main sewers as well as the surcharged sewer pipes.

Once the characteristics of a sewer network are known, the above equations could be used to estimate the overall CH_4 emission from the entire sewer network, with an assumption that all the CH_4 produced in the sewer network ultimately gets emitted to the atmosphere. Although, there have been some efforts made towards the validation of these models, more work is needed.

8.2.5 Methane emission in sewers

The mass transfer of CH_4 from the liquid phase to the sewer headspace is the key process for CH_4 emission. Like oxygen, the mechanism of CH_4 liquid-gas mass transfer in assumed to be controlled by the transfer in the liquid film as, similarly to oxygen, methane is poorly soluble in water. The following relationship is commonly used for modelling the liquid-gas transfer of methane.

$$\frac{dC_{CH4,L}}{dt} = -k_L a \cdot \left(C_{CH4,L} - \frac{C_{CH4,g}}{H} \right) \tag{8.7}$$

where $k_L a$ is the mass transfer coefficient (1/day); $C_{CH4,L}$ is the liquid phase methane concentration (mg/L); $C_{CH4,g}$ is the methane concentration in the gas phase (mg/L); H is the Henry's law constant; and $dC_{CH4,L} / dt$ is the volumetric mass flux of methane (mg/L·day).

The mass transfer coefficient depends upon several factors including temperature, water quality and the thickness of the interfacial liquid layer (Liss & Slater, 1974). A number of different relationships are available for the estimation of the $k_L a$ value for oxygen transfer as a function of physical and hydraulic properties of sewer pipes and streams (Jensen, 1995; Lahav *et al.*, 2004; Owens *et al.*, 1964; Parkhurst & Pomeroy, 1972). Once the mass transfer coefficient for oxygen is known, the same for methane could be estimated based on the ratio of the coefficient of molecular diffusion of CH_4 to that of O_2 (Liss & Slater, 1974) as follows.

$$\frac{k_L a, CH_4}{k_L a, O_2} = \left(\frac{D_{CH_4}}{D_{O_2}} \right)^n \tag{8.8}$$

where $k_L a, CH_4$ is the mass transfer coefficient for CH_4; $k_L a, O_2$ is the mass transfer coefficient for O_2; D_{CH_4} is the molecular diffusion coefficient for CH_4; D_{O_2} is the molecular diffusion coefficient for O_2; and n is the constant, which could be taken as 0.5 under turbulent flow conditions (Liss & Slater, 1974; Carrera *et al.*, 2016).

8.2.6 Model calibration and validation

There has been some work done in relation to calibrating and validating the methane models for the collection system (Chaosakul *et al.*, 2014; Foley *et al.*, 2009; Liu *et al.*, 2015a). However, only a limited data set (either from a single system or data over a limited period) has been used in the calibration, and hence the validity of the model parameters is questionable. It is therefore warranted that the models are calibrated with the data collected from the field and such a calibrated model be applied to estimate the methane generation in and emission from a sewer network.

Different models presented in previous sections would require different data sets for their calibration. Generally, sewer data (pipe size, slope, length etc.), hydraulic data (flow, velocity, water depth, pump operation information etc.), environmental data (temperature etc.), and wastewater characteristics are required as inputs for the calibration. The empirical models require quantification of the parameters and variables involved in the model and generally use average values for the variables, whereas a dynamic model would require the information on dynamic variation of flow and the wastewater characteristics. For comparison, dissolved CH_4 concentration needs to be monitored at selected locations along the sewer network. This data can be used for both calibration and validation of the model. Normally data collected from one system is used for calibration of model parameters and the data from a separate system is used for validation.

8.2.7 Further model development

Liu *et al.* (2015a) have highlighted the limitations of the current CH_4 models for sewer CH_4 production. For instance, the potential for biological CH_4 oxidation has not been factored in in the current models mainly because of the lack of understanding of those processes. In addition, other processes which serve as a sink for methane in sewers should be included in the models once such processes are identified and a proper understanding is established.

Another potential development is related to the integrated management of urban water-wastewater systems as there is an increasing interest in understanding the effect of the interactions among urban water system components. This can be enabled through integrating the WWTP model and the sewer models, such as SeweX, resulting in better prediction of methane emission over the entire wastewater system (Guo *et al.*, 2012). With further development of the sewer models, the integrated modelling approach will provide more reliable information in relation to GHG emissions from the entire urban water system.

8.3 METHANE MODELLING FOR ACTIVATED SLUDGE PROCESS

8.3.1 Incorporating aerobic methane oxidation in activated sludge models

Because of the aerobic environment prevailing in the activated sludge process, the only process that is relevant to methane emission is the aerobic methane oxidation due to the presence of methanotrophs. The well-established Activated Sludge Model n°1 (ASM1, Henze *et al.*, 1987) has been extended by Daelman *et al.* (2014) to include the biological methane oxidation. The resulting model, named ASM1m, adds two processes to ASM1: aerobic growth and decay of methanotrophs. The two additional state variables in the model are methane as a substrate (S_{CH4}) and methane oxidizing bacteria (X_{MOB}) as the biomass component. Methanotrophic bacteria are singled out from the other heterotrophic organisms (X_{BH}) and are therefore described by a separate state variable, X_{MOB}, as in Arcangeli and Arvin (1999). The details of the reaction stoichiometry and kinetic parameters used in ASM1m are available in Arcangeli and Arvin (1999) and Daelman *et al.* (2014). The original parameter values of ASM1 are preserved and the list has been extended with additional parameters to be used in the equations that describe methanotrophic growth and decay, taken from Arcangeli and Arvin (1999). The details of the reaction stoichiometry and the process rates used in ASM1m model are presented in Tables 8.2 and 8.3, respectively.

In ASM1m, the growth of methanotrophs is modelled using Monod kinetics for methane and oxygen similar to those used in a number of publications (Alvarez-Cohen & McCarty, 1991; Arcangeli & Arvin, 1999; Broholm *et al.*, 1992; Oldenhuis *et al.*, 1991; Yoon *et al.*, 2009). Unlike in Yoon *et al.* (2009), oxygen is also considered as a limiting substrate. Ammonia inhibition, as considered by Arcangeli and Arvin (1999), is not included in the model.

The effect of the ammonium concentration on the methane oxidation rate by methanotrophs is ambiguous. A number of studies have reported an inhibitory effect of ammonium (Begonja & Hrsak, 2001; Hanson & Hanson, 1996; Nyerges & Stein, 2009), while others have reported no such effect (van der Ha *et al.*, 2010, 2011). In contrast, Noll *et al.* (2008) observed selective stimulation of methanotrophs by ammonium. These observations have been made under ammonium concentrations at least one order of magnitude higher than the concentration commonly encountered in an activated sludge system and in systems described in models such as BSM1. Ammonium inhibition is therefore omitted in the model. Decay of methanotrophic biomass is described in the same manner as the other biomass groups, using the concept of death-regeneration. First-order reaction kinetics has been used for the biomass decay.

8.3.2 Modelling methane gas-liquid mass transfer

The modelling of gas-liquid transfer of methane is illustrated considering a completely mixed reactor, with the reactor influent as the sole source of methane, dissolved methane leaving with the effluent, methane stripping (transfer from the liquid to the gas phase) and biological methane conversion (Figure 8.5).

A typical mass balance for dissolved methane, m_{CH4} (g COD) then reads as Equation (8.9).

$$\frac{dm_{CH4}(t)}{dt} = Q_{in}(t) \cdot S_{CH4,in}(t) - Q_{out}(t) \cdot S_{CH4}(t) - \dot{m}_{CH4}^{L\text{-}G(t)} - \dot{R}_{CH4(t)} \tag{8.9}$$

Q_{in} and Q_{out} (m³/d) are the imposed liquid flows into and out of the reactor, respectively, $S_{CH4,in}$ and S_{CH4} (g COD/m³) are the respective incoming and outgoing methane concentrations, $\dot{m}_{CH4}^{L\text{-}G}$ (g COD/d) is the stripping rate and $\dot{R}_{CH4}$ (g COD/d) is the conversion rate. The concentration of methane in the liquid volume, V (m³), relates to its total mass via Equation (8.10).

$$S_{CH4}(t) = \frac{m_{CH4}(t)}{V(t)} \tag{8.10}$$

It is important to realize that the liquid-gas transfer rate, $\dot{m}_{CH4}^{L\text{-}G}$, is affected by gradients in the gas phase composition and pressure, which can be taken into account through comprehensive expressions

Table 8.2 Matrix representation of ASM1m (Daelman *et al.*, 2014). The processes and reactions added to the original ASM1 are shaded.

A_{ij}	S_I gCOD/m³	S_S gCOD/m³	S_{CH4} gCOD/m³	X_I gCOD/m³	X_S gCOD/m³	X_{BH} gCOD/m³	X_{BA} gCOD/m³	X_{MOB} gCOD/m³	X_P gCOD/m³	S_O gCOD/m³	S_{NO} gN/m³	S_{NH} gN/m³	S_{ND} gN/m³	X_{ND} gN/m³	S_{ALK} mole HCO₃⁻/m³
PROCESS							STOICHIOMETRIC MATRIX								
1. Aerobic growth of heterotrophs		$-1/Y_H$				1				$-(1-Y_H)/Y_H$		$-i_{XB}$			$-i_{XB}/14$
2. Anoxic growth of heterotrophs		$-1/Y_H$				1					$-(1-Y_H)/(2.86 Y_H)$	$-i_{XB}$			$(1-Y_H)/(14\times2.86\times Y_H) -i_{XB}/14$
3. Aerobic growth of autotrophs							1			$-(4.57-Y_A)/Y_A$	$1/Y_A$	$-i_{XB}-1/Y_A$			$-i_{XB}/14-1/(7\times Y_A)$
4. Aerobic growth of methanotrophs			$-1/Y_{MOB}$					1		$-(1-Y_{MOB})/Y_{MOB}$		$-i_{XB}$			$-i_{XB}/14$
5. Decay of heterotrophs					$1-f_P$	-1			f_P					$i_{XB}-f_P\times i_{XP}$	
6. Decay of autotrophs					$1-f_P$		-1		f_P					$i_{XB}-f_P\times i_{XP}$	
7. Decay of methanotrophs					$1-f_P$			-1	f_P					$i_{XB}-f_P\times i_{XP}$	
8. Ammonification of soluble organic nitrogen												1	-1		$1/14$
9. Hydrolysis of entrapped organics		1			-1										
10. Hydrolysis of entrapped organic nitrogen													1	-1	
CONSERVATIVES							COMPOSITION MATRIX								
COD	1	1	1	1	1	1	1	1	1	-1	-4.57	0			
N						i_{XB}	i_{XB}	i_{XB}	i_{XP}	0	1	1	1	1	
Charge											$-1/14$	$1/14$			-1

Table 8.3 Process rates for ASM1m (Daelman *et al.*, 2014). The rates for the processes added to the original ASM1 are shaded.

j	Process	Process Rate (ρ_j)
1.	Aerobic growth of heterotrophs	$\mu_H^{max} \cdot \dfrac{S_S}{K_S + S_S} \cdot \dfrac{S_O}{K_O^H + S_O} \cdot X_{BH}$
2.	Anoxic growth of heterotrophs	$\mu_H^{max} \cdot \dfrac{S_S}{K_S + S_S} \cdot \dfrac{K_O^H}{K_O^H + S_O} \cdot \dfrac{S_{NO}}{K_{NO} + S_{NO}} \cdot \eta_{y.g} \cdot X_{BH}$
3.	Aerobic growth of autotrophs	$\mu_A^{max} \cdot \dfrac{S_{NH}}{K_{NH}^A + S_{NH}} \cdot \dfrac{S_O}{K_O^A + S_O} \cdot X_{BA}$
4.	Aerobic growth of methanotrophs	$\mu_{MOB}^{max} \cdot \dfrac{S_{CH4}}{K_{NH4} + S_{CH4}} \cdot \dfrac{S_O}{K_O^{MOB} + S_O} \cdot X_{MOB}$
5.	Decay of heterotrophs	$b_H \cdot X_{BH}$
6.	Decay of autotrophs	$b_A \cdot X_{BA}$
7.	Decay of methanotrophs	$b_{MOB} \cdot X_{MOB}$
8.	Ammonification of soluble organic nitrogen	$k_a \cdot S_{ND} \cdot X_{BH}$
9.	Hydrolysis of entrapped organics	$k_H \cdot \dfrac{X_S / X_{BH}}{K_X + X_S / X_{BH}} \cdot \left[\dfrac{S_O}{K_O^H + S_O} + \eta_{y.h} \cdot \dfrac{K_O^H}{K_O^H + S_O} \cdot \dfrac{S_{NO}}{K_{NO} + S_{NO}} \right] \cdot X_{BH}$
10.	Hydrolysis of entrapped organic nitrogen	$k_H \cdot \dfrac{X_S / X_{BH}}{K_X + X_S / X_{BH}} \cdot \left[\dfrac{S_O}{K_O^H + S_O} + \eta_{y.h} \cdot \dfrac{K_O^H}{K_O^H + S_O} \cdot \dfrac{S_{NO}}{K_{NO} + S_{NO}} \right] \cdot X_{BH} \cdot \dfrac{X_{ND}}{X_S}$

(Baeten *et al.*, 2020). However, in the case of methane, the stripping rate can be very well approximated with a liquid-gas transfer model (Equation (8.11)) that considers the mean gas phase mole fraction and mean pressure along the reactor height (Baeten *et al.*, 2020).

$$\dot{m}_{CH4}^{L\text{-}G(t)} = K_{La_{O2(t)}} \cdot V(t) \cdot \frac{S_{CH4}(t) - i_{COD,CH4} \cdot h_{CH4} \cdot \left(\left(\left(p_{atm}^{G+pg}(H/2) \right) M_{CH4} \right) / RT \right) \cdot x_{in,CH4}^G}{\sqrt{(D_{O2} / D_{CH4}) + 0.6} \cdot h_{CH4} \cdot (H/2)} \tag{8.11}$$
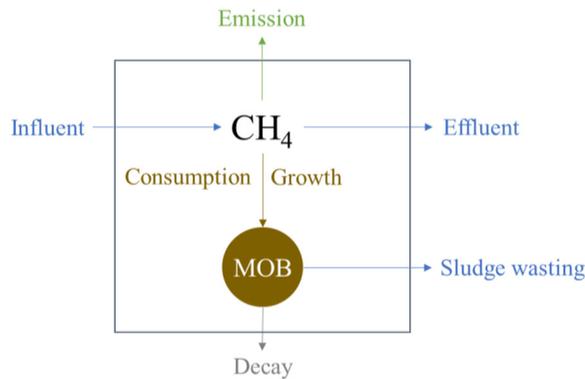
Figure 8.5 Sinks and sources of methane (CH_4) and methane oxidizing bacteria (MOB) considered in a simple completely stirred tank reactor (CSTR) model (Baeten *et al.*, 2021).

$K_L a_{O2}$ (1/d) denotes the volumetric overall transfer coefficient of oxygen, $i_{COD,CH4}$ (g COD/g) is the COD content of methane, h_{CH4} (g/m^3 in the liquid phase per g/m^3 in the gas phase) is the Henry coefficient of methane, p_{atm}^G (Pa) is the atmospheric pressure, ρ (kg/m^3) is the density of water, g (m/s^2) is the gravitational acceleration, H (m) is the water column height during aeration, M_{CH4} (g/mol) is the molecular mass of methane, R (J/mol·K) is the universal gas constant, T is the reactor temperature (K), $x_{in,CH4}^G$ (mole/mole) is the mole fraction of methane in the atmosphere and D_{O2} and D_{CH4} (m^2/d) are the respective diffusion coefficients of oxygen and methane.

8.4 METHANE MODELLING FOR ANAEROBIC DIGESTION

Anaerobic Digestion Model No. 1 (ADM1), developed and published by IWA Anaerobic Digestion Modelling Task Group (Batstone *et al.*, 2002), is widely used as the model for methane production and emission during anaerobic digestion. The model considers disintegration and hydrolysis, acidogenesis, acetogenesis and methanogenesis steps.

ADM1 comprises a large number of simultaneous and sequential processes with a complex reaction kinetics. The processes are primarily classified as either biochemical or physicochemical. The biochemical reactions are considered to be catalysed by extra-cellular enzymes involving organic substrates. Empirical based first-order reaction kinetics is used for all the extra-cellular biochemical reactions, while all the intra-cellular biochemical reactions follow the Monod-type kinetics. Typical to any biological reaction, substrate uptake reaction rates are considered to be a function of the biomass growth rate and biomass concentration. The model considers pH inhibition for acetogenic and acetolactic methanogenic bacterial groups through H$_2$ and free ammonia inhibition, respectively.

The details of the processes, kinetic expressions, and stoichiometric and kinetic parameters used in the model are available in IWA (2002). Since ADM1 has been widely reported in the literature, no further description has been provided in this chapter.

REFERENCES

Alvarez-Cohen L. and McCarty P. L. (1991). Product toxicity and cometabolic competitive-inhibition modeling of chloroform and trichloroethylene transformation by methanotrophic resting cells. *Applied and Environmental Microbiology*, **57**(4), 1031–1037. https://doi.org/10.1128/aem.57.4.1031-1037.1991

Arcangeli J. P. and Arvin E. (1999). Modelling the growth of a methanotrophic biofilm: estimation of parameters and variability. *Biodegradation*, **10**(3), 177–191. https://doi.org/10.1023/A:1008317906069

Baeten J. E., van Loosdrecht M. C. M. and Volcke E. I. P. (2020). When and why do gradients of the gas phase composition and pressure affect liquid-gas transfer? *Water Research*, **178**, 115844. https://doi.org/10.1016/j.watres.2020.115844

Baeten J. E., Walgraeve C., Granja R., van Loosdrecht M. C. M. and Volcke E. I. P. (2021). Unaerated feeding alters the fate of dissolved methane during aerobic wastewater treatment. *Water Research*, **204**, 117619. https://doi.org/10.1016/j.watres.2021.117619

Batstone D. J., Keller J., Angelidaki I., Kalyuzhnyi S. V., Pavlostathis S. G., Rozzi A., Sanders W. T. M., Siegrist H. and Vavilin V. A. (2002). The IWA anaerobic digestion model no 1 (ADM1). *Water Science and Technology*, **45**(10), 65–73. https://doi.org/10.2166/wst.2002.0292

Begonja A. and Hrsak D. (2001). Effect of growth conditions on the expression of soluble methane monooxygenase. *Food Technology and Biotechnology*, **39**(1), 29–35.

Broholm K., Christensen T. H. and Jensen B. K. (1992). Modeling TCE degradation by a mixed culture of methane-oxidizing bacteria. *Water Research*, **26**(9), 1177–1185. https://doi.org/10.1016/0043-1354(92)90178-7

Carrera L., Springer F., Lipeme-Kouyi G. and Buffiere P. (2016). A review of sulfide emissions in sewer networks: overall approach and systemic modelling. *Water Science and Technology*, **73**(6), 1231–1242.

Cesca J., Sharma K., Vuong L., Yuan Z., Hamer G. and McDonald A. (2015). South Australia Water Corporation's pro-active corrosion and odour management strategy development. *Proceedings of the Water Environment Federation*, **2015**(9), 919–935. https://doi.org/10.2175/193864715819555463

Chaosakul T., Koottatep T. and Polprasert C. (2014). A model for methane production in sewers. *Journal of Environmental Science and Health, Part A*, **49**, 1316–1321. https://doi.org/10.1080/10934529.2014.910071

Daelman M. R. J., Van Eynde T., van M. C. M. and Volcke E. I. P. (2014). Effect of process design and operating parameters on aerobic methane oxidation in municipal WWTPs. *Water Research*, **66**, 308–319. https://doi.org/10.1016 j.watres.2014.07.034

Foley J., Yuan Z. and Lant P. (2009). Dissolved methane in rising main sewer systems: field measurements and simple model development for estimating greenhouse gas emissions. *Water Science & Technology*, **60**, 2963–2971. https://doi.org/10.2166/wst.2009.718

Guisasola A., Sharma K. R., Keller J., Yuan Z. and Jiang G. (2009). Development of a model for assessing methane formation in rising main sewers. *Water Research*, **43**, 2874–2884. https://doi.org/10.1016/j.watres.2009.03.040

Guo L., Porro J., Sharma K. R., Amerlinck Y., Benedetti L., Nopens I., Shaw A., Van Hulle S. W. H., Yuan Z. and Vanrolleghem P. A. (2012). Towards a benchmarking tool for minimizing wastewater utility greenhouse gas footprints. *Water Science & Technology*, **66**, 2483–2495. https://doi.org/10.2166/wst.2012.495

Hanson R. S. and Hanson T. E. (1996). Methanotrophic bacteria. *Microbiological Reviews*, **60**(2), 439–471. https://doi.org/10.1128/mr.60.2.439-471.1996

Henze M., Grady C. P. L. J., Gujer W., Marais G. v. R. and Matsuo T. (1987). Activated Sludge Model No. 1, IAWQ Scientific and Technical Report No. 1, IAWQ, London.

IWA Task Group for Mathematical Modelling of Anaerobic Digestion Processes (2002). Anaerobic Digestion Model No.1 (ADM1), IWA Scientific and Technical Report, IWA Publishing, London

Jensen N. A. (1995). Empirical modeling of air-to-water oxygen transfer in gravity sewers. *Water Environment Research*, **67**(6), 979–991. https://doi.org/10.2175/106143095X133211

Lahav O., Lu Y., Shavit U. and Loewenthal R. (2004). Modeling hydrogen sulphide emission rates in gravity sewage collection systems. *Journal of Environmental Engineering*, **130**(11), 1382–1389. https://doi.org/10.1061/(ASCE)0733-9372(2004)130:11(1382)

Liss P. S. and Slater P. G. (1974). Flux of gases across the air-sea interface. *Nature*, **247**(5438), 181–184. https://doi.org/10.1038/247181a0

Liu Y., Ni B. J., Sharma K. R. and Yuan Z. (2015a). Methane emission from sewers. *Science of the Total Environment*, **524–525**, 40–51. https://doi.org/10.1016/j.scitotenv.2015.04.029

Liu Y., Sharma K. R., Fluggen M., O'Halloran K., Murthy S. and Yuan Z. (2015b). Online dissolved methane and total dissolved sulfide measurement in sewers. *Water Research*, **68**, 109–118. https://doi.org/10.1016/j.watres.2014.09.047

Liu Y., Tugtas A. E., Sharma K. R., Ni B. J. and Yuan Z. (2016). Sulfide and methane production in sewer sediments: field survey and model evaluation. *Water Research*, **89**, 142–150. https://doi.org/10.1016/j.watres.2015.11.050

Mohanakrishnan J., Gutierrez O., Sharma K. R., Guisasola A., Werner U., Meyer R. L., Keller J. and Yuan Z. (2009). Impact of nitrate addition on biofilm properties and activities in rising main sewers. *Water Research*, **43**, 4225–4237. https://doi.org/10.1016/j.watres.2009.06.021

Nguyen T., Sharma K., Jiang G., Ganigue R., Cesca J., Vuong L. and Yuan Z. (2015). SeweX modelling to support corrosion and odour management in sewers. *Water (Journal of Australian Water Association)*, **42**(7), 71–78.

Noll M., Frenzel P. and Conrad R. (2008). Selective stimulation of type I methanotrophs in a rice paddy soil by urea fertilization revealed by RNA-based stable isotope probing. *Fems Microbiology Ecology*, **65**(1), 125–132. https://doi.org/10.1111/j.1574-6941.2008.00497.x

Nyerges G. and Stein L. Y. (2009). Ammonia cometabolism and product inhibition vary considerably among species of methanotrophic bacteria. *FEMS Microbiology Letters*, **297**(1), 131–136. https://doi.org/10.1111/j.1574-6968.2009.01674.x

Oldenhuis R., Oedzes J. Y., Vanderwaarde J. J. and Janssen D. B. (1991). Kinetics of chlorinated hydrocarbon degradation by Methylosinus trichosporium OB3B and toxicity of trichloroethylene. *Applied and Environmental Microbiology*, **57**(1), 7–14. https://doi.org/10.1128/aem.57.1.7-14.1991

Owens M., Edwards E. W. and Gibbs J. W. (1964). Some reaeration studies in streams. *International Journal of Air Pollution*, **8**, 469–486.

Parkhurst J. D. and Pomeroy R. D. (1972). Oxygen absorption in streams. *Journal of the Sanitary Engineering Division, ASCE*, **98**(SA1), 101–124. https://doi.org/10.1061/JSEDAI.0001366

Schierbaum K. D., Weimar U. and Göpel W. (1992). Comparison of ceramic, thick-film and thin-film chemical sensors based upon SnO_2. *Sensors & Actuators B Chemical*, **7**, 709–716. https://doi.org/10.1016/0925-4005(92)80390-J

Sharma K., de Haas D., Corrie S., O'Halloran K., Keller J. and Yuan Z. (2008). Predicting hydrogen sulfide formation in sewers: a new model. *Water*, **35**, 132–137.

van der Ha D., Hoefman S., Boeckx P., Verstraete W. and Boon N. (2010). Copper enhances the activity and salt resistance of mixed methane-oxidizing communities. *Applied Microbiology and Biotechnology*, **87**(6), 2355–2363. https://doi.org/10.1007/s00253-010-2702-4

van der Ha D., Bundervoet B., Verstraete W. and Boon N. (2011). A sustainable, carbon neutral methane oxidation by a partnership of methane oxidizing communities and microalgae. *Water Research*, **45**(9), 2845–2854. https://doi.org/10.1016/j.watres.2011.03.005

Willis J., Yuan Z., Sharma K., Jiang G., Murthy S., DeClippelleir H., Kumar A. and Satyadev A. (2020). Conveyance Asset Prediction System: Sewer Methane Estimation Methodology and Significance Determination, The Water Research Foundation, USA.

Xu J., He Q., Li H., Yang C., Wang Y. and Ai H. (2018). Modelling of methane formation in gravity sewer system: the impact of microorganism and hydraulic condition. *AMB Express*, **8**(1), 1–10.

Yoon S., Carey J. N. and Semrau J. D. (2009). Feasibility of atmospheric methane removal using methanotrophic biotrickling filters. *Applied Microbiology and Biotechnology*, **83**(5), 949–956. https://doi.org/10.1007/s00253-009-1977-9

NOMENCLATURE

α	Temperature coefficient
ADM1	Anaerobic Digestion Model No. 1
A/V	Sewer biofilm area to water volume ratio
ASM1	Activated Sludge Model 1
$C_2H_4O_2$	Acetate
$C_3H_6O_2$	Propionate
$C_6H_{12}O_6$	Glucose
C_{CH4}	Dissolved methane concentration
$C_{CH4,L}$	Liquid phase methane concentration
$C_{CH4,g}$	Gas phase methane concentration
CH_4	Methane
CO_2	Carbon di-oxide
CSTR	Completely stirred tank reactor
D	Pipe diameter
D_{CH4}	Molecular diffusion coefficient for CH_4
D_{O_2}	Molecular diffusion coefficient for O_2
GHG	Greenhouse gases
H	Henry's law constant
H_2	Hydrogen gas
H_2O	Water
H_2S	Hydrogen sulfide
H_2SO_4	Sulfuric acid
HRT	Hydraulic residence time
IWA	International Water Association

k	Rate constant for methane production
k_{CH_4,H_2}	Rate constant for methane production with hydrogen
$k_{CH_4,SAC}$	Rate constant for methane production with acetate
k_{H_2S,H_2}	Rate constant for sulfide production with hydrogen
$k_{H_2S,PROP}$	Rate constant for sulfide production with propionate
$k_{H_2S,SAC}$	Rate constant for sulfide production with acetate
$k_L a_{,CH_4}$	Mass transfer coefficient for CH_4
$k_L a_{,O_2}$	Mass transfer coefficient for O_2
$K_{AC,SRB}$	Half saturation constant for acetate (sulfidogenesis)
K_F	Half saturation constant for fermentable substrate
$K_{H_2,MA}$	Half saturation constant for hydrogen (methanogenesis)
$K_{H_2,SRB}$	Half saturation constant for hydrogen (sulfidogenesis)
$K_{PROP,SRB}$	Half saturation constant for propionate (sulfidogenesis)
$K_{SAC,MA}$	Half saturation constant for acetate (methanogenesis)
K_{SO_4}	Half saturation constant for sulfate (sulfidogenesis)
N_P	Number of pumping events per day
O_2	Oxygen
P_I	Average pumping interval
q_{ACETOG}	Rate constant for acetogenesis
q_{ACIDOG}	Rate constant for acidogenesis
Q	Average daily flow rate
Q_{CH4}	Methane production
r_{CH4}	Methane production rate
S	Pipe slope
S_{AC}	Acetate concentration
S_{CH_4}	Dissolved methane concentration
S_F	Fermentable substrate concentration
S_{H_2}	Hydrogen concentration
S_{PROP}	Propionate concentration
SRB	Sulfate reducing bacteria
S_{SO_4}	Sulfate concentration
T	Wastewater temperature (°C)
X	Amount of biomass
X_{BA}	Autotrophic biomass concentration
X_{BH}	Heterotrophic biomass concentration
X_{MOB}	Concentration of methane oxidizing bacteria
$Y_{CH4/}x$	Yield coefficient (mg CH_4/kg biomass)